The effects of Cowling's approximation on adiabatic wave propagation for radially symmetric backgrounds in helioseismology

Lola Chabat, Florian Faucher, Ha Pham, Hélène Barucq, Damien Fournier

The effects of Cowling's approximation on adiabatic wave propagation for radially symmetric backgrounds in helioseismology

Lola Chabat[1,*], **Florian Faucher**[1], **Ha Pham**[1], **Hélène Barucq**[1], **Damien Fournier**[2]

[1]Project-Team Makutu, Inria, University of Pau and Pays de l'Adour, TotalEnergies, CNRS, France.
[2]Max Planck Institute for Solar System Research, Göttingen, Germany

[*]Email: lola.chabat@inria.fr

Abstract

In this work, to model acoustic solar waves, we solve the equations derived by Lynden-Bell & Ostriker (1967) under spherical symmetry. These equations contain gravity effects in form of background gravitation and its perturbation δ_ϕ which is commonly neglected in Cowling's approximation. Radial symmetry is exploited to reduce the problem to a system of modal equation decoupled on each harmonic mode and implement exact Dirichlet-to-Neumann(DtN) condition for δ_ϕ. In comparing the performance between Hybridizable Discontinuous Galerkin (HDG) and Continuous Galerkin (CG) methods, we show that HDG is more robust with regard to mesh refinement than CG. Our numerical solution to Dirac response contains peaks whose positions agree with the location of eigenvalues computed with sofware GYRE.

Keywords: Helioseismology, Cowling's approximation, DtN, Galbrun's equation, HDG

1 Introduction

In this work, with $\mathbb{B}_{\rm S} = \{|\mathbf{x}| \leq r_b\}$ representing solar interior, we investigate the problem having as unknown Lagrangian displacement $\boldsymbol{\xi}$ and the gravitational potential perturbation δ_ϕ:

$$\begin{cases} -(\sigma^2\rho_0 + \boldsymbol{\mathcal{L}})\boldsymbol{\xi} + \rho_0\nabla\delta_\phi = \mathbf{F}, & \text{on } \mathbb{B}_{\rm S}, \\ \Delta\delta_\phi = \begin{cases} -4\pi G\,\nabla\cdot(\rho_0\boldsymbol{\xi})\,, & \text{on } \mathbb{B}_{\rm S}, \\ 0 & \text{on } \mathbb{R}^3\setminus\mathbb{B}_{\rm S}, \end{cases} \end{cases} \tag{1}$$

with operator $\boldsymbol{\mathcal{L}}$ defined as

$$\begin{aligned}\boldsymbol{\mathcal{L}}\boldsymbol{\xi} = \nabla(\gamma\, p_0\nabla_{\mathbf{x}}\cdot\boldsymbol{\xi}) - (\nabla p_0)(\nabla_{\mathbf{x}}\cdot\boldsymbol{\xi}) + \nabla[(\boldsymbol{\xi}\cdot\nabla)p_0] \\ - \ (\boldsymbol{\xi}\cdot\nabla)\nabla p_0 \ - \ \rho_0\,(\boldsymbol{\xi}\cdot\nabla_{\mathbf{x}})\,\nabla\phi_0,\end{aligned}$$

with p_0 the pressure, ρ_0 the density, γ the adiabatic index, ϕ_0 the gravitational potential satisfying

$$\Delta\phi_0 = 4\pi G\rho_0\,, \quad \phi_0 \to 0,\ |\mathbf{x}|\to\infty\,.$$

This is coupled with boundary conditions,

$$\{\mathfrak{B}\boldsymbol{\xi} = 0 \ \text{ on } \partial\mathbb{B}_{\rm S};\ \ \delta_\phi \to 0 \ \text{ as } \mathbf{x}\to\infty \tag{2}$$

Here $\mathfrak{B}$ represents a finite-domain type boundary condition for $\boldsymbol{\xi}$. In this work, we assume the background parameters are radially symmetric and follow standard solar model S.

We solve Problem (1)-(2) using HDG and CG. We show that HDG is numerically more robust to accommodate the model S background and discontinuous source in the Poisson equation (1). The model S background presents a challenge for numerical resolution due to the rapid decrease of density and sound speed near the surface. We also need to investigate the position of the artificial boundary, denoted by $r_{\max}$ at which DtN condition (2) is imposed. For HDG, we will also need to construct a choice of stabilization. All of the subsequent simulations have been performed using `hawen` [2].

2 Modal equations

Following [1] which considers the system (1) with Cowling approximation, radial symmetry is exploited to decouple the problem (1) + (2) on each spherical harmonic mode ℓ to give a system of ordinary differential equations in radial variable. It is further reduced to a system having as unknown the coefficients of the radial displacement $\boldsymbol{\xi}$ and δ_ϕ in spherical harmonics,

$$\boldsymbol{\xi}\cdot\mathbf{e}_r = \sum_{\ell=0}^{\infty}\sum_{m=-\ell}^{\ell} a_\ell^m Y_\ell^m, \ \ \delta_\phi = \sum_{\ell=0}^{\infty}\sum_{m=-\ell}^{\ell} d_\ell^m\, Y_\ell^m.$$

With $\mathfrak{f}_\ell$, $\mathfrak{g}_\ell$ depending on the coefficients of $\mathbf{F}$ in vector spherical harmonic basis, (a_ℓ^m, d_ℓ^m) satisfies for each (m,ℓ),

$$\begin{cases} (\hat{q}_\ell\partial_r^2 + q_\ell\partial_r + \tilde{q}_\ell)a_\ell + \Big(Q\,\partial_r + \tilde{Q}\Big)\,d_\ell = \mathfrak{f}_\ell, \\ (r^2\partial_r^2 + 2r\partial_r + \tilde{m}_\ell)d_\ell + (Pr\partial_r + \tilde{P})a_\ell = \mathfrak{g}_\ell. \end{cases} \tag{3}$$

Coefficients of the above ODE depend on physical parameters. We employ the exact DtN condition for d_ℓ at $r = r_{\max}$ and a free-surface or a

Dirichlet condition at $r = r_b$ for a_ℓ

$$\begin{cases} r a'_\ell = 0\,, \quad r d'_\ell + \ell d_\ell = 0 & \text{at } r = 0; \quad (4a) \\ r\, d'_\ell + (\ell+1) d_\ell = 0 & \text{on } r = r_{\max}; \quad (4b) \\ \alpha\, r\, a'_\ell + a_\ell = 0 & \text{on } r = r_b. \quad (4c) \end{cases}$$

The equation (4b) is the exact DtN which replaces condition $\delta_\phi \to 0$ at infinity. In (4c) $\alpha = 0$ corresponds to $\boldsymbol{\xi} \cdot \mathbf{n} = 0$, while $\alpha = 1/(-2 + \frac{\alpha_{p_0}}{\gamma} r)$ is the free-surface condition $\delta_p = 0$. (4a) chooses regular solution at $r = 0$.

3 Numerical results

Position of artificial boundary DtN condition (4b) has to be placed disjoint with support of the source of the Poisson equation, i.e. $r_{\max} = r_b + \epsilon$ where $\epsilon > 0$. In our tests, we use $r_{\max} = 1.1$.

Stabilization In HDG method, a definition for the numerical Neumann trace has to be given:

$$\widehat{r\partial_r a} = r\partial_r a_h + \tau_a(a_h - \lambda_a)\,, \quad (5)$$

$$\widehat{r\partial_r d} = r\partial_r d_h + \tau_d(d_h - \lambda_d)\,, \quad (6)$$

with stabilization factors denoted τ_a, τ_d. For τ_a, we work with the Schrödinger form of the ODE in Cowling approximation (i.e., without d_ℓ), $-\partial_r^2 + V_\ell$, to infer

$$\tau_a = -r\left(\frac{\mathfrak{J}'_\ell}{\mathfrak{J}_\ell} - \mathrm{i}\sqrt{-V_\ell}\,\nu\right). \quad (7)$$

Here $\nu = 1$ for right end-point $\nu = -1$ for left end-point. $\mathfrak{J}_\ell$ appears in the change of variable to obtain Schrödinger form and depends on physical background and ℓ [1]. The stabilization for d_ℓ is obtained in a similar fashion,

$$\tau_d = 1 - \sqrt{\ell(\ell+1)}\,\nu\,, \quad \text{for } \ell > 0, \quad (8)$$

$$\tau_d = (1 - \nu\, r)\,, \quad \text{for } \ell = 0. \quad (9)$$

3.1 Comparison between HDG and CG

The two methods of discretization are compared on two meshes. Mesh M1 contains refinement around $r = 1$ due to the complexity of near-surface layers of Model S. Mesh M2 is obtained from M1 by further refinement in the neighborhood of $r = r_b$. The comparison is shown in Figure 1 in terms of solutions a_ℓ obtained with HDG or CG and on these two meshes. We see that CG requires mesh M2 which is more refined around $r = r_b$, while HDG is robust and shows the same result on both meshes.

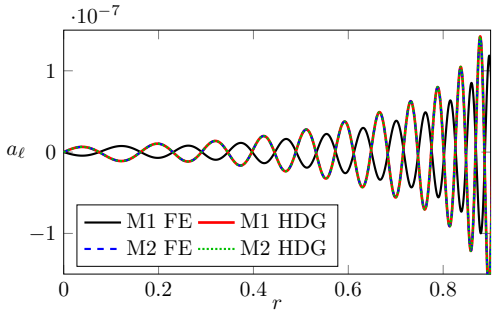

Figure 1: Comparison between HDG and CG on two different meshes showing solution a_ℓ at $\ell = 2$, $\omega/2\pi = 5$ mHz, with HDG showing agreement on both meshes.

3.2 Comparison with Gyre

In comparing Green's functions with and without Cowling's approximation, we observe the theoretically predicted shifts in the locations of maximum power of these two solutions, which reduce as ℓ increases, as shown in Figure 2. Additionally, since peaks in magnitude indicate the position of an eigenvalue, in superposing our solution with eigenvalues computed by software GYRE by (Townsend & Teitler (2013)), we find agreement between the location of peaks of our solution and Gyre's eigenvalues.

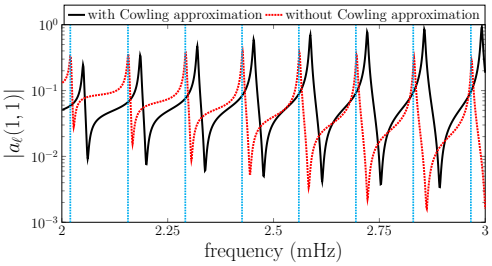

Figure 2: Solution $a_\ell(1, 1, \omega)$ with and without the Cowling approximation, in superposition with eigenvalues computed by Gyre represented by vertical lines.

References

[1] H. Barucq, F. Faucher, D. Fournier, L. Gizon and H. Pham. Outgoing modal solutions for Galbrun's equation in helioseismology. *JDE*, (2021).

[2] F. Faucher. `hawen`: time-harmonic wave modeling and inversion using HDG. *JOSS*, (2021).